

Multimodal Generative Models for Scalable Weakly-Supervised Learning

Mike Wu¹ Noah Goodman¹

Abstract

Multiple modalities often co-occur when describing natural phenomena. Learning a joint representation of these modalities should yield deeper and more useful representations. Previous work have proposed generative models to handle multi-modal input. However, these models either do not learn a joint distribution or require complex additional computations to handle missing data. Here, we introduce a multimodal variational autoencoder that uses a product-of-experts inference network and a sub-sampled training paradigm to solve the multi-modal inference problem. Notably, our model shares parameters to efficiently learn under any combination of missing modalities, thereby enabling weakly-supervised learning. We apply our method on four datasets and show that we match state-of-the-art performance using many fewer parameters. In each case our approach yields strong weakly-supervised results. We then consider a case study of learning image transformations—edge detection, colorization, facial landmark segmentation, etc.—as a set of modalities. We find appealing results across this range of tasks.

1. Introduction

Learning from diverse modalities has the potential to yield more abstract and generalizable representations. For instance, the visual appearance and tactile impression of an object give very different information that converges on a more invariant abstract representation (Yildirim, 2014). Similarly, an image and a textual description can capture complimentary but converging information about a scene (Vinyals et al., 2015; Xu et al., 2015). As these examples illustrate, modalities often differ greatly in structure—both raw format and the statistical disposition of information.

¹Department of Computer Science, Stanford University, Palo Alto, California, USA. Correspondence to: Mike Wu <wu-mike@cs.stanford.edu>.

Thus any model able to usefully represent inter-modal information will be highly non-linear. Recent literature relies on deep neural networks to act as a bridge between modalities (Ngiam et al., 2011; Srivastava and Salakhutdinov, 2012).

Learning a general multi-modal model is difficult because multi-modal data is *expensive* and *sparse*. Often we are in a *weakly supervised* setting of having only a small set of examples with all observations present, but having access to a larger dataset with one (or a subset of) modalities. Ideally, we wish to engineer a model that is robust to such a pattern of missing data so that we can bootstrap learning from existing uni-modal corpora and a small set of complete multi-modal examples.

We propose a multimodal variational autoencoder (MVAE), an extension of the VAE framework (Kingma and Welling, 2013). The generative model, from latent variables to observations, in the traditional VAE is trained jointly with an *inference network* from observations to latents by optimizing the evidence lower bound (ELBO). To do this in the multi-modal case, we would require an inference network for each modality: $q(z|x_1)$, $q(z|x_2)$, ..., $q(z|x_N)$, and for each combination of modalities: $q(z|x_1, x_2)$, $q(z|x_3, x_4, x_5)$, $q(z|x_1, x_2, ..., x_n)$, etc. To avoid an exponential number of inference networks, we *share parameters* via a product-of-experts (Hinton, 2006). However, if we naively trained this product-of-experts on data points that contain all modalities, it would insufficiently constrain the individual modality inference networks (essentially because a product underdetermines its factors). We instead treat multi-modal data as also providing uni-modal examples, updating the ELBO for both the joint and individual modalities on each gradient step. This combination of product-of-experts inference networks with sub-sampled training provides a novel and useful solution to the multi-modal inference problem that also immediately enables learning from weak (uni-modal) data.

We report a series of experiments to compare our model to similar approaches. Following recent literature, we train on MNIST (LeCun et al., 1998), binarized MNIST (Larochelle and Murray, 2011), MultiMNIST (Eslami et al., 2016; Sabour et al., 2017), FashionMNIST (Xiao et al., 2017), and CelebFaces and Attributes (CelebA) (Liu et al., 2015). Several of these datasets have complex modalities—

character sequences, RGB images—requiring large inference networks with RNNs and CNNs. We show that our model is able to support heavy encoders with thousands of parameters. On each dataset our model learns a good generative model of the data, matching state-of-the-art performance in terms of data log-likelihood. We further explore the quality of the inference networks learned in each case, finding that ours have significantly lower variance when used as importance distributions for their models.

By treating the 18 attributes of CelebA as individual modalities (rather than jointly as a single modality) we begin to explore how our model extends to a larger number of modalities, finding better performance from sharing of statistical strength. We further explore this question by choosing several image transformations commonly studied in computer vision—colorization, edge detection, segmentation, etc.—and synthesizing a dataset by applying them to CelebA. We show that a single generative model can jointly learn all the above transformations by modeling them as modalities.

Finally, we investigate how our model performs under weak supervision by aggressively reducing the number of multimodal examples we provide to the model. We see that the MVAE is able to learn a good joint representation when only 1% of examples are multi-modal for simpler datasets and 10% for more complex datasets. This suggests that the MVAE can be feasibly used for real-world tasks by ‘bootstrapping’ from uni-modal data.

In summary, the contributions of this paper are as follows: First, we describe a product-of-experts scheme for deriving inference networks in a multimodal setting (similar to a recent proposal by (Vedantam et al., 2017)). Second, we present an efficient and scalable training paradigm. Third, we explore learning with more than two modalities. Finally, we show that MVAEs perform well at weakly-supervised learning, with no changes required to support arbitrary combinations of missing data.

2. Methods

We first recall the variational autoencoder, then extend to the multimodal setting.

2.1. Variational Autoencoders

A variational autoencoder (VAE) (Kingma and Welling, 2013) is a latent variable generative model of the form $p_\theta(x, z) = p(z)p_\theta(x|z)$ where $p(z)$ is a prior, usually Gaussian. The decoder, $p_\theta(x|z)$, consists of a deep neural net, with parameters θ , composed with a simple likelihood (e.g. Bernoulli or Gaussian). The goal of training is to maximize the marginal likelihood of the data (the “evidence”), however since this is intractable, the evidence lower bound (ELBO) is instead optimized. The ELBO is defined via

an inference network, $q_\phi(z|x)$, which serves as a tractable importance distribution:

$$E_{q_\phi(z|x)}[\lambda \log p_\theta(x|z)] - \beta \text{KL}[q_\phi(z|x), p(z)], \quad (1)$$

where $\text{KL}[p, q]$ is the Kullback-Leibler divergence between distributions p and q ; β (Higgins et al., 2016) and λ are weights balancing the terms in the ELBO. In practice, $\lambda = 1$ and β is slowly annealed to 1 to form a valid lower bound on the evidence.

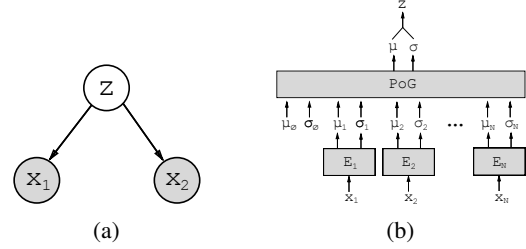


Figure 1. (a) Graphical model of the MVAE. Gray circles represent observed variables. (b) Structure of N inference networks given N modalities. E_i represents the i -th inference network; μ_i and σ_i represent the i -th variational (Gaussian) parameters; μ_0 and σ_0 represent the prior expert parameters. The product-of-experts (PoE) combines all variational parameters in a principled and efficient manner. If a modality is missing during training, we drop the respective inference network, falling back to the prior expert if no data is present. Thus, the parameters of E_1, \dots, E_N are shared across different combinations of missing inputs.

2.2. Multimodal Variational Autoencoders

A multimodal variational autoencoder (MVAE) uses a generative model of the form $p_\theta(x_1, x_2, \dots, x_N) = p(z)p_\theta(x_1|z)p_\theta(x_2|z) \cdots p_\theta(x_N|z)$ where x_1, \dots, x_N are N different modalities and z is a common latent variable (Fig. 1a). The ELBO becomes:

$$E_{q_\phi(z|x_{1...N})} \left[\sum_{i=1}^N \lambda_i \log p_\theta(x_i|z) \right] - \beta \text{KL}[q_\phi(z|x_{1...N}), p(z)], \quad (2)$$

where λ_i and β allow different modalities (or the prior) to be differentially weighted.

If we did not allow missing data at either training or test, we could simply train this model as a VAE. In order to make the MVAE robust to missing data, we have to solve two problems: how to define 2^N inference networks (e.g. $q_\phi(z|x_1)$, $q_\phi(z|x_1, x_3)$, etc), and how to ensure that these inference networks are sufficiently trained.

2.3. Product of Experts Inference Networks

In order to define 2^N inference networks without an exponential explosion in the number of parameters that must be

trained, we assume a product of experts structure (Hinton, 2006). For any subset $X \subseteq \{x_1, \dots, x_N\}$, we define the joint inference network $q(z|X)$ as:

$$q(z|X) \propto p(z) \prod_{x_i \in X} q(z|x_i), \quad (3)$$

where a prior expert, $p(z)$ is added as a form of regularization. This defines all of the multi-modality inference networks from the N uni-modal $q_\phi(z|x_i)$ (Fig. 1b). Fortunately, because each expert is Gaussian, the product is itself Gaussian (Cao and Fleet, 2014). The resulting distribution has mean $\mu = (\sum_i \mu_i \Sigma_i^{-1}) (\sum_i \Sigma_i^{-1})^{-1}$ and covariance $\Sigma = (\sum_i \Sigma_i^{-1})^{-1}$, where μ_i, Σ_i are the mean and (diagonal) covariance of the i -th Gaussian expert.

In the presence of missing modalities during training, the ELBO (Eqn. 4) generalizes naturally, using the product-of-gaussians inference network defined by the modalities present. If we write a data point as the collection of modalities present, that is $X = \{x_i | i^{th} \text{ modality present}\}$, then the ELBO becomes:

$$E_{q_\phi(z|X)} \left[\sum_{x_i \in X} \lambda_i \log p_\theta(x_i|z) \right] - \beta \text{KL}[q_\phi(z|X), p(z)]. \quad (4)$$

2.4. Sub-sampled Training Paradigm

A product of Gaussians does not uniquely specify its component Gaussians. Hence, training using the above objective has an unfortunate consequence when there are no missing modalities: we never train the individual inference networks (or small sub-networks) and thus do not know how to use them at test time. To get around this issue, we propose a simple training scheme. We sub-sample the modalities present in each training example, treating complete examples as also providing partial data.

In particular, if we have a data point X with M modalities, then we include an ELBO term for each of the 2^M subsets $Y \subset X$. Training using every combination of partial data requires only M encoders but requires evaluating 2^M ELBO terms in the MVAE objective. In practice, evaluating loss terms is much cheaper than training additional inference networks. However, to reduce the cost further, we sub-sample the available loss terms. Specifically, we evaluate (1) the ELBO using the product of all M gaussians, (2) all ELBO terms using a single modality, and (3) k ELBO terms using k randomly chosen subsets. At each gradient step, we thus evaluate a different subset of the 2^M ELBO terms. In expectation, we will be approximating the full MVAE objective. We explore the effect of k in Section .

A pleasant side-effect of this training scheme is that it immediately applies to weakly-supervised training, where $M < N$, the total number of modalities.

3. Related Work

Many variants of VAEs (Kingma and Welling, 2013; Kingma et al., 2014) have been used to train generative models of the form $p(y|x)$, including conditional VAEs (CVAE) (Sohn et al., 2015) and conditional multimodal autoencoders (CMMA) (Pandey and Dukkipati, 2017). Notably, these models are not bi-directional. We are more interested in studying models where we can condition interchangeably.

For example, the BiVCCA (Wang et al., 2016) trains two VAEs together with interacting inference networks such that we can reconstruct in either direction. However, it does not attempt to explicitly learn the joint distribution, sacrificing expressivity for simplicity. We find empirically that modeling $p(x, y)$ significantly improves the ability of the model to capture the data distribution.

Several recent models have tried to capture the joint distribution explicitly, many of which share elements with the MVAE. Suzuki et al. (2016) introduce the joint multimodal VAE (JMVAE), which learns $p(x, y)$ using a joint inference network, $q(z|x, y)$. To handle missing data at test time, the JMVAE collectively trains the joint encoder with two additional inference networks $q(z|x)$ and $q(z|y)$. The authors use an ELBO objective with two extra KL divergence terms to minimize the distance between the uni-modal and the multi-modal inference networks. Compared to the MVAE, the JMVAE trains a new inference network for each multi-modal subset, requiring 2^N inference networks for N modalities and corresponding extra terms in the objective.

Most recently, Vedantam et al. (2017) introduce another objective for the bi-modal VAE, which they call the *triplet ELBO*. The authors use the objective to learn abstract concepts in a compositional hierarchy. Like the MVAE, their model’s joint inference network $q(z|x, y)$ combines variational distributions using a product-of-experts rule. Unlike the MVAE, the authors report a two-stage training process: using complete data, fit $q(z|x, y)$ and the decoders. Then, freezing $p_{\theta_x}(x|z)$ and $p_{\theta_y}(y|z)$, fit the uni-modal inference networks, $q(z|x)$ and $q(z|y)$ to handle missing data. Because training is separated, the model has to fit an exponential number of inference networks to handle all subsets of missing data in stage two. In contrast, the MVAE only needs a linear number of inference networks. To the best of our knowledge, the MVAE is the first deep generative model to explore more than 2 modalities efficiently. Moreover, the single-stage training of the MVAE makes it uniquely applicable to weakly-supervised learning.

4. Experiments

As in previous literature, we transform commonplace uni-modal datasets into multi-modal problems by treating the labels as a second modality. We also construct a MultiMNIST

dataset where the second modality is a string of digit labels. We compare existing models (VAE, BiVCCA, JMVAE) to the MVAE and show that we equal state-of-the-art performance. For each dataset, we keep the inference network and decoder architectures consistent across different models, varying only the objective and training procedure.

4.1. MNIST/BinaryMNIST

We use the MNIST hand-written digits dataset (LeCun et al., 1998) where digit labels are treated as a separate modality. We use 50k examples for training, 10k validation, 10k testing. We also train on a binarized version of MNIST to align with previous literature.

Training Details As done in Suzuki et al. (2016), we use the Adam optimizer (Kingma and Ba, 2014) with a learning rate of 10^{-3} , a minibatch size of 100, 64 latent dimensions, and train for 500 epochs. We set $\lambda = 1$, and anneal β from 0 to 1 linearly for the first 200 epochs.

For the image encoder, $q(z|x)$ and decoder, $p(x|z)$ we use an MLP with two hidden layers of 512 nodes with Swish non-linearity (Ramachandran et al., 2017). For the text encoder $q(z|y)$ and decoder $p(y|z)$, we use a continuous embedding layer of size 10, and a two layer MLP, again with 512 nodes and Swish. We model $p(x|z)$ with a Bernoulli likelihood and $p(y|z)$ with a Multinomial likelihood over the vocabulary of 10.

Model	BinaryMNIST	MNIST	FashionMNIST	MultiMNIST	CelebA
VAE	730240	730240	3409536	1316936	4070472
CVAE	735360	735360	3414656	—	4079688
BiVCCA	1063680	1063680	3742976	1841936	4447504
JMVAE	2061184	2061184	7682432	4075064	9052504
MVAE	1063680	1063680	3742976	1841936	4447504
JMVAE19	—	—	—	—	3.6259e12
MVAE19	—	—	—	—	10857048

Table 1. Number of Inference Network Parameters for each generative model. For a single dataset, each generative model uses the same inference network architecture(s) for each modality. Thus, the difference in parameters is solely due to how the modalities interact in the model. We note that MVAE has the same number of parameters as BiVCCA. JMVAE19 and MVAE19 show the number of parameters using 19 inference networks when each of the attributes in CelebA is its own modality.

4.2. FashionMNIST

This is an MNIST-like fashion product dataset containing 28 x 28 grayscale images of clothing from 10 classes—skirts, shoes, sweatshirts, t-shirts, etc (Xiao et al., 2017). This dataset is intended to be more difficult than MNIST.

Training Details We use identical hyperparameters for training as in MNIST. However, we employ a miniature

DCGAN architecture (Radford et al., 2015) for the image encoder and decoder using two convolutional and two deconvolutional layers respectively.

Estimating $\log p(x)$ using $q(z x)$					
Model	BinaryMNIST	MNIST	FashionMNIST	MultiMNIST	CelebA
VAE	-86.313	-91.126	-232.758	-152.835	-6237.120
BiVCCA	-87.354	-92.089	-233.634	-202.490	-7263.536
JMVAE	-86.305	-90.697	-232.630	-152.787	-6237.967
MVAE	-86.026	-90.619	-232.535	-152.761	-6236.923
MVAE19	—	—	—	—	-6236.109
Estimating $\log p(x, y)$ using $q(z x)$					
JMVAE	-86.371	-90.769	-232.948	-153.101	-6242.187
MVAE	-86.255	-90.859	-233.007	-153.469	-6242.034
MVAE19	—	—	—	—	-6239.944
Estimating $\log p(x y)$ using $q(z x)$					
CVAE	-83.448	-87.773	-229.667	—	-6228.771
JMVAE	-83.985	-88.696	-230.396	-145.977	-6231.468
MVAE	-83.970	-88.569	-230.695	-147.027	-6234.955
MVAE19	—	—	—	—	-6233.340

Table 2. Estimates for log marginal, log joint, and log conditional probabilities on the average test example using $q(z|x)$ as an importance distribution. We estimate these values using 1000 particles. MVAE and JMVAE are about equivalent in data log-likelihood but as Table 1 shows, MVAE uses far fewer parameters.

4.3. MultiMNIST

This is another variant of MNIST where between 0 and 4 digits are composed together on a 50x50 canvas. Unlike Eslami et al. (2016), the digits in our MultiMNIST dataset are located in four fixed locations. Provided a MultiMNIST image, we generate the text modality by concatenating the digit classes from top-left to bottom-right. This is much more difficult than MNIST due to variable length text (the ‘labels’) and more complex images. We again use 50k for training, 10k for validation, 10k for testing.

Training Details We use the same hyperparameters as in MNIST. However, we use 100 latent dimensions for z . For the image encoder and decoder, we use the DCGAN architecture from Radford et al. (2015). For the text encoder, we use a continuous embedding layer of size 10, followed by a bidirectional GRU with 200 hidden units, and a single fully-connected layer to project into the latent dimension. For the text decoder, we include a start token and a stop token in the vocabulary. Generating text is as follows: provided a start token, compute its continuous embedding, feed it through a fully-connected layer, then a two-layer GRU, followed by another fully-connected layer and a softmax over the 12 character space. We sample a new character and repeat until generating a stop token. We note that previous work has not explored RNN inference networks in multi-modal learning, which we show to work well with our model.

Estimating $\log p(x)$ using $q(z x, y)$					
Model	BinaryMNIST	MNIST	FashionMNIST	MultiMNIST	CelebA
JMVAE	-86.234	-90.962	-232.401	-153.026	-6234.542
MVAE	-86.051	-90.616	-232.539	-152.826	-6237.104
MVAE19	—	—	—	—	-6236.113
Estimating $\log p(x, y)$ using $q(z x, y)$					
JMVAE	-86.304	-91.031	-232.700	-153.320	-6238.280
MVAE	-86.278	-90.851	-233.007	-153.478	-6241.621
MVAE19	—	—	—	—	-6239.957
Estimating $\log p(x y)$ using $q(z x, y)$					
JMVAE	-83.820	-88.436	-230.651	-145.761	-6235.330
MVAE	-83.940	-88.558	-230.699	-147.009	-6235.368
MVAE19	—	—	—	—	-6233.330

Table 3. Similar estimates as in Table 2 but using $q(z|x, y)$ as an importance distribution (instead of $q(z|x)$). Because VAE and CVAE do not have a multi-modal inference network, they are excluded from this table.

4.4. CelebA

The large-scale CelebFaces Attributes (CelebA) dataset (Yang et al., 2015) contains over 200k images of celebrities. Each image is tagged with 40 attributes i.e. wears glasses, or has bangs. We use the aligned and cropped version with a selected 18 visually distinctive attributes, as done in Perarnau et al. (2016). Images are rescaled to 64x64. Training and testing splits are replicated as in Yang et al. (2015).

For CelebA, MVAE treats images as one modality and attributes as a second modality where a single inference network predicts all 18 attributes. We also explore a variation of MVAE, called MVAE19, where we treat each attribute as its own modality for a total of 19. To approximate the full objective for MVAE19, we set $k = 1$ i.e. we use all single-modality terms, the complete 19-modality term, and randomly sample one term from the total space of 2^{19} possible terms for an objective with 21 ELBO terms.

Training Details We use Adam with a learning rate of 10^{-4} , a minibatch size of 100, and train for 100 epochs with linear KL annealing for the first 20 epochs. We use 100 latent dimensions. We use the same image encoders and decoders as in MultiMNIST but with 3 input channels. We use an MLP with 2 hidden layers of size 512 with batch normalization and Swish as the attribute encoder and decoder. For MVAE19, we have 18 such encoders and decoders.

5. Evaluation

For two-modality cases (all except MVAE19), we measure the test marginal log-likelihood, $\log p(x)$, and test joint log-likelihood $\log p(x, y)$ using 100 importance samples in CelebA and 1000 samples in other datasets. We compute the log of the estimated evidence $\log p(x)$ based on which encoder is used to generate variational parameters:

$$\log p(x) \approx \log E_{q_{\phi_x}(z|x)} \left[\frac{p_{\theta_x}(x|z)p(z)}{q_{\phi_x}(z|x)} \right] \quad (5)$$

$$\log p(x) \approx \log E_{q_{\phi_{xy}}(z|x, y)} \left[\frac{p_{\theta_x}(x|z)p(z)}{q_{\phi_{xy}}(z|x, y)} \right] \quad (6)$$

We can approximate two estimates for $\log p(x, y)$ in a similar fashion. We can also estimate the test conditional log-likelihood $\log p(x|y)$, as a measure of classification performance, as done in Suzuki et al. (2016):

$$\log p(x|y) \approx \log E_{q_{\phi_y}(z|y)} \left[\frac{p_{\theta_x}(x|z)p_{\theta_y}(y|z)p(z)}{q_{\phi_y}(z|y)} \right] - \log E_{p_z} [p_{\theta_y}(y|z)] \quad (7)$$

In MNIST, FashionMNIST, and MultiMNIST, we use 5000 samples to estimate the second expectation in Equation 7. In CelebA, we use 1000 samples.

Finally, we compare the quality of the inference networks learned. In all VAE-based models, the inference network functions as an importance distribution for approximating the intractable posterior. A better importance distribution, which more accurately approximates the posterior, results in importance weights with lower variance. Thus, we compute the variance of the (log) importance weights for each distribution of interest (e.g. $\log \frac{p_{\theta_x}(x|z)p(z)}{q_{\phi_x}(z|x)}$).

6. Results

Figure 2 shows image samples and conditional image samples for each dataset using the image generative model, $p(x|z)$ and sampling from either $z \sim p(z)$ or $z \sim q(z|y)$. Good quality images are generated for each domain, and conditional images x are largely correctly matched to the target label/text y .

Tables 2 and 3 compare test log-likelihoods for MVAE and for previous models using either $q(z|x)$ or $q(z|x, y)$ as the inference network for importance sampling.¹ We see that MVAE performs on par with the state-of-the-art (JMVAE) while using far fewer parameters (Table 1) via sharing of inference networks. When considering only $p(x)$ (i.e. the likelihood of the image modality alone), the MVAE also performs as well or better than the VAE, indicating that solving the harder multi-modal problem does not sacrifice any uni-modal model capacity. On CelebA, MVAE19 (which treats features as independent modalities) consistently outperforms the MVAE (which treats the feature vector as a single modality). This suggests that the PoE approach generalizes well to a larger number of modalities, and that jointly training modalities shares some statistical strength.

Tables 4 and 5 show variances of log importance weights using $q(z|x)$ and $q(z|x, y)$, respectively. We see that in the majority of datasets, MVAE produces lower variance than

¹Because importance sampling with either $q(z|x)$ or $q(z|x, y)$ yields an unbiased estimator of marginal likelihood, we expect the log-likelihoods in Tables 2 and 3 to agree asymptotically.

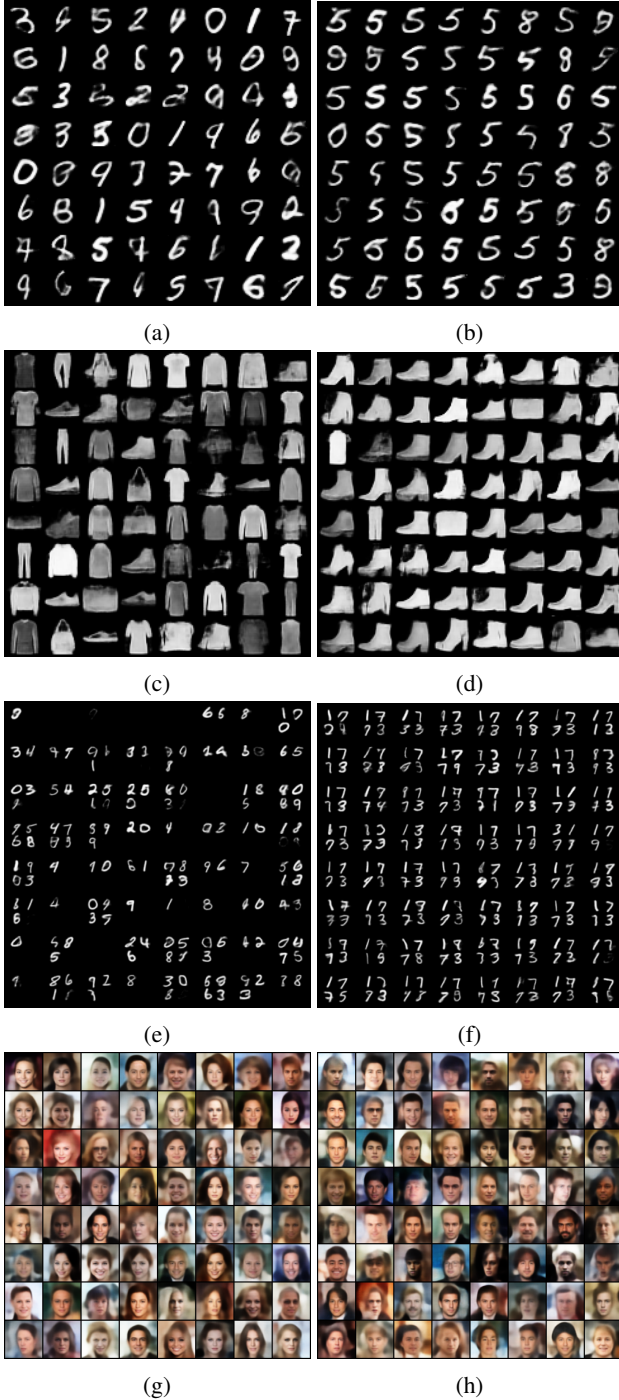


Figure 2. Image Samples using MVAE. (a, c, e, g) show 64 images per dataset by sampling $z \sim p(z)$ and then generating via $p(x|z)$. Similarly, (b, d, f, h) show conditional image reconstructions by sampling $z \sim q(z|y)$ where (b) $y = 5$, (d) $y = \text{Ankle boot}$, (f) $y = 1773$, (h) $y = \text{Male}$ followed by generation.

other methods, implying a better inference network. Furthermore, MVAE19 consistently produces lower variance than MVAE in CelebA.

Variance of Marginal Log Importance Weights: $\text{var}(\log(\frac{p(x,z)}{q(z x)}))$					
Model	BinaryMNIST	MNIST	FashionMNIST	MultiMNIST	CelebA
VAE	22.264	26.904	25.795	54.554	56.291
BiVCCA	55.846	93.885	33.930	185.709	429.045
JMVAE	39.427	37.479	53.697	84.186	331.865
MVAE	22.181	25.640	20.309	26.917	73.923
MVAE19	—	—	—	—	71.640
Variance of Joint Log Importance Weights: $\text{var}(\log(\frac{p(x,y,z)}{q(z x,y)}))$					
JMVAE	41.003	40.126	56.640	91.850	334.887
MVAE	23.343	27.570	20.587	27.989	72.030
MVAE19	—	—	—	—	—
Variance of Conditional Log Importance Weights: $\text{var}(\log(\frac{p(x,z y)}{q(z x,y)}))$					
CVAE	21.203	22.486	12.748	—	56.852
JMVAE	23.877	26.695	26.658	37.726	81.190
MVAE	19.478	25.899	18.443	16.822	73.885
MVAE19	—	—	—	—	71.824

Table 4. Average variance of log importance weights for marginal, joint, and conditional distributions using $q(z|x)$. 1000 importance samples were used to approximate the variance. The lower the variance, the better quality the inference network.

Variance of Marginal Log Importance Weights: $\text{var}(\log(\frac{p(x,z)}{q(z x,y)}))$					
Model	BinaryMNIST	MNIST	FashionMNIST	MultiMNIST	CelebA
JMVAE	22.387	24.962	28.443	35.822	80.808
MVAE	21.791	25.741	18.092	16.437	73.871
MVAE19	—	—	—	—	71.546
Variance of Joint Log Importance Weights: $\text{var}(\log(\frac{p(x,y,z)}{q(z x,y)}))$					
JMVAE	23.309	26.767	29.874	38.298	81.312
MVAE	21.917	26.057	18.263	16.672	74.968
MVAE19	—	—	—	—	71.953
Variance of Conditional Log Importance Weights: $\text{var}(\log(\frac{p(x,z y)}{q(z x,y)}))$					
JMVAE	40.646	40.086	56.452	92.683	335.046
MVAE	23.035	27.652	19.934	28.649	77.516
MVAE19	—	—	—	—	71.603

Table 5. Average variance of log importance weights for marginal, joint, and conditional distributions using $q(z|x, y)$.

Finally, in the case of more than two modalities, there is a question of how the number of sampled ELBO terms (k) affects the model’s performance. To investigate, we vary k from 0 to 50 and train MVAE19 on the CelebA dataset, each with 100 latent states. As seen in Figure 3, increasing k has little effect on data log-likelihood (estimated with 1000 importance samples), but reduces the variance of the importance distribution defined by the inference networks. In practice, we choose $k = 1$ as a tradeoff between compute time and variance of the importance distribution.

6.1. Weak Supervision

For each of the four datasets, we investigate weakly-supervised training by randomly reserving only a fraction of the dataset as multi-modal examples. The remaining data is split into two datasets: one with only the first modality, and one with only the second. We then vary the fraction of multi-modal data (supervision) and examine effects on the predictive task $p(y|x)$, e.g. predict the correct digit label from an MNIST image. The total number of examples

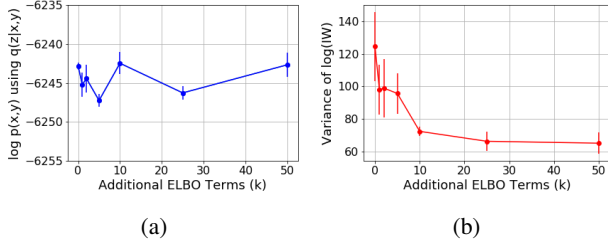


Figure 3. Effect of approximating the MVAE objective with more terms on (a) the joint log-likelihood and (b) the variance of the log importance weights. (a) shows that using $k = 0$ (meaning only $N + 1$ ELBO terms) performs roughly the same as $k = 50$; however, (b) shows that switching from $k = 0$ to $k = 1$ greatly reduces the variance in the importance distribution defined by the inference network(s). (a) and (b) are plotted over 3 separate trials.

shown to the model is always fixed – only the proportion of paired bi-modal examples is varied.

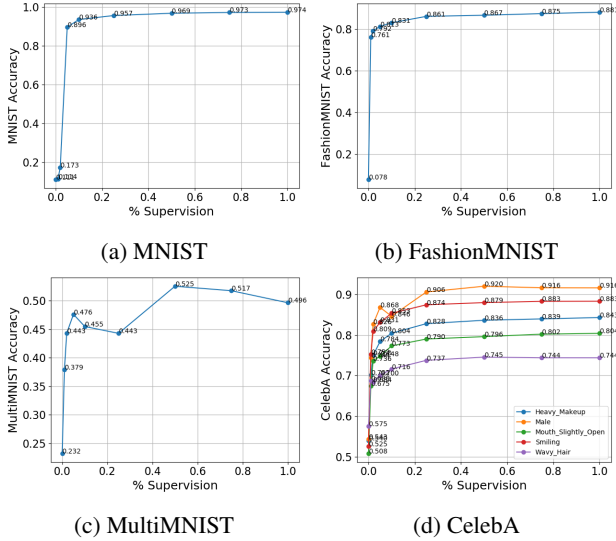


Figure 4. Effects of Supervision Level. We plot the level of supervision as a fraction from 0 (meaning that no paired examples were provided during training) to 1 (meaning no missing modalities) against the accuracy on a prediction task. For (a) MNIST (non-binarized) and (b) FashionMNIST, we predict the target class. For (c) MultiMNIST, we predict 0 to 4 characters describing the digits in an image. Figure (c) shows the accuracy for predicting each character correctly. For (d) CelebA, we predict each attribute independently. We use the MVAE19 model and either observe all attributes or none. Because many attributes are imbalanced, (d) only shows 5 attributes where the prediction task is not trivial.

Figure 4 shows the effect of exposure to more multi-modal examples during training on accuracy. We see a diminishing marginal return across all datasets, suggesting that given a small set of multi-modal examples, we can still effectively learn the joint distribution using a larger set of uni-modal

data. For example, in smaller datasets like MNIST and FashionMNIST, just 1% of multi-modal examples is sufficient to achieve near full-supervision performance. In CelebA and MultiMNIST, around 10% is sufficient.

For MVAE19 on CelebA, we can conduct a different weak supervision experiment: given a complete multi-modal example (x_1, \dots, x_{19}) , randomly keep x_i with probability p for each $i = 1, \dots, 19$. Doing so for all examples in the training set, we simulate the effect of missing modalities beyond the bi-modal setting. Here, the number of examples shown to the model is dependent on p e.g. $p = 0.5$ suggests that on average, 1 out of every 2 x_i are dropped. We vary p from 0.001 to 1, train from scratch, and plot (1) the prediction accuracy per attribute and (2) the various data log-likelihoods. From Figure 5, we conclude that the method is fairly robust to missing data. Even with $p = 0.1$, we still see accuracy close to the prediction accuracy with full data.

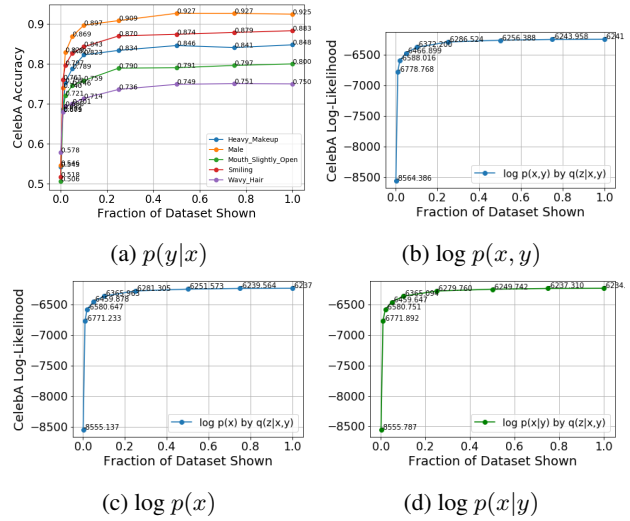


Figure 5. Effects of Missing Training Data. Using the CelebA dataset, we randomly drop input features x_i with probability p . Figure (a) shows the effect of increasing p from 0.001 to 1 on the average accuracy of sampling the correct attribute given an image. Figure (b) and (c) show changes in log marginal and log conditional approximations as p increases. In all cases, we see close-to-best performance using only 10% of the data.

7. Case study: Computer Vision Applications

In this section, we apply popular image processing tools to CelebA and show that we can learn these transformations (and their inverses) as conditional distributions using MVAE. In particular, we focus on the following: colorization, edge detection, facial landmark segmentation, image completion, and watermark removal (see Figure 6). Reconstructing the original image is itself a modality for a total of six.

To construct the dataset, we manually apply ground-truth

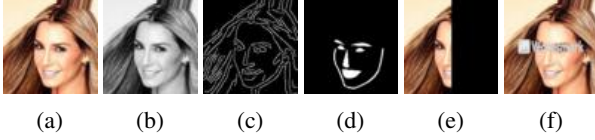


Figure 6. *Samples from Modified CelebA Dataset*: The MVAE is given a set of 6 images during training: (a) the original CelebA image, (b) a grayscale image, (c) an edge-detected image, (d) a facial landscape mask, (e) an obscured image, and (f) a watermarked image. The images shown here have been rescaled to 64x64.

transformations to each image in the corpus. For *colorization*, we transform RGB colors to grayscale. For *image completion*, half of the image is replaced with black pixels. And for *watermark removal*, we overlay a fixed generic watermark from Google Images on the input image. For the more complex operations, we rely on off-the-shelf tools: we use the default Canny edge detection (Canny, 1987) from Scikit-Image (Van der Walt et al., 2014) to extract edges; we use dlib (King, 2009) and OpenCV (Bradski and Kaehler, 2000) for computing facial landscape masks.

We fit the MVAE with 250 latent dimensions using the MVAE objective (with $k=1$, $N=6$) and the sub-sampled training paradigm detailed above. We use Adam with a 10^{-4} learning rate, a batch size of 50, $\lambda_i = 1$ for all i , β annealing for 20 epochs and train for 100 epochs.

Figures 7, 8, 9, 10 plot eight samples each showcasing a different learned transformation. For Figure 7 we encode the original image with the learned encoder, then decode the transformed image with the learned generative model. We see reasonable reconstruction, and good facial landscape and edge extraction. For Figures 8, 9, 10 we go in the opposite direction, encoding a transformed image and then sampling from the generative model to reconstruct the original. The results are quite good: reconstructed half-images agree on gaze direction and hair color, colorizations are reasonable, and all trace of the watermark is removed. (Though the reconstructed images still suffer from the same blurriness that VAEs do (Zhao et al., 2017).) These results show the usefulness of jointly modeling the different modalities. Like the weak supervision experiments above, learning image transformations in this manner is robust to missing data.

8. Conclusion

In this paper, we introduced a multi-modal variational autoencoder with a new training paradigm that learns a joint distribution, allows bidirectional sampling, and is robust to missing data during training and testing. By optimizing the ELBO with multi-modal and uni-modal examples, we fully utilize the product-of-experts structure to share inference network parameters in a fashion that scales to an arbi-



Figure 7. *Edge Detection and Facial Landscapes*: The top row shows 8 ground truth images randomly chosen from the CelebA dataset. The second to fourth rows respectively plot the reconstructed image, edge, and facial landscape masks using the trained MVAE decoders and $q(z|x_1, \dots, x_6)$.



Figure 8. *Colorization*: The top row shows ground truth grayscale images. The bottom row show reconstructed color images.

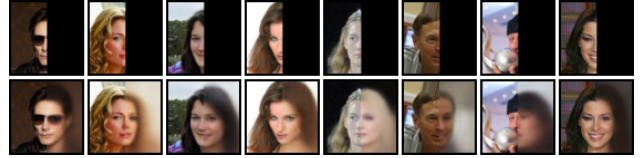


Figure 9. *Fill in the Blank*: The top row shows ground truth CelebA images with half of each image obscured. The bottom row replaces the obscured part with a reconstruction.



Figure 10. *Removing Watermarks*: The top row shows ground truth CelebA images, each with an added watermark. The bottom row shows the reconstructed image with the watermark removed.

trary number of modalities. In our experiments, the MVAE matches state-of-the-art performance in data log-likelihoods across four bi-modal datasets. We also demonstrate the power of our method on two truly *multi*-modal datasets: CelebA with each attribute as its own modality, and a number of popular image processing techniques. In future work, we would like to explore a product of mixture of Gaussian posteriors, and apply our method to more real-world tasks, such as image captioning and tactile-visual learning.

References

- G. Bratski and A. Kaehler. Opencv. *Dr. Dobbs journal of software tools*, 3, 2000.
- J. Canny. A computational approach to edge detection. In *Readings in Computer Vision*, pages 184–203. Elsevier, 1987.
- Y. Cao and D. J. Fleet. Generalized product of experts for automatic and principled fusion of gaussian process predictions. *arXiv preprint arXiv:1410.7827*, 2014.
- S. A. Eslami, N. Heess, T. Weber, Y. Tassa, D. Szepesvari, G. E. Hinton, et al. Attend, infer, repeat: Fast scene understanding with generative models. In *Advances in Neural Information Processing Systems*, pages 3225–3233, 2016.
- I. Higgins, L. Matthey, A. Pal, C. Burgess, X. Glorot, M. Botvinick, S. Mohamed, and A. Lerchner. beta-vae: Learning basic visual concepts with a constrained variational framework. 2016.
- G. E. Hinton. Training products of experts by minimizing contrastive divergence. *Training*, 14(8), 2006.
- D. E. King. Dlib-ml: A machine learning toolkit. *Journal of Machine Learning Research*, 10(Jul):1755–1758, 2009.
- D. P. Kingma and J. Ba. Adam: A method for stochastic optimization. *arXiv preprint arXiv:1412.6980*, 2014.
- D. P. Kingma and M. Welling. Auto-encoding variational bayes. *arXiv preprint arXiv:1312.6114*, 2013.
- D. P. Kingma, S. Mohamed, D. J. Rezende, and M. Welling. Semi-supervised learning with deep generative models. In *Advances in Neural Information Processing Systems*, pages 3581–3589, 2014.
- H. Larochelle and I. Murray. The neural autoregressive distribution estimator. In *Proceedings of the Fourteenth International Conference on Artificial Intelligence and Statistics*, pages 29–37, 2011.
- Y. LeCun, L. Bottou, Y. Bengio, and P. Haffner. Gradient-based learning applied to document recognition. *Proceedings of the IEEE*, 86(11):2278–2324, 1998.
- Z. Liu, P. Luo, X. Wang, and X. Tang. Deep learning face attributes in the wild. In *Proceedings of International Conference on Computer Vision (ICCV)*, 2015.
- J. Ngiam, A. Khosla, M. Kim, J. Nam, H. Lee, and A. Y. Ng. Multimodal deep learning. In *Proceedings of the 28th international conference on machine learning (ICML-11)*, pages 689–696, 2011.
- G. Pandey and A. Dukkipati. Variational methods for conditional multimodal deep learning. In *Neural Networks (IJCNN), 2017 International Joint Conference on*, pages 308–315. IEEE, 2017.
- G. Perarnau, J. van de Weijer, B. Raducanu, and J. M. Álvarez. Invertible conditional gans for image editing. *arXiv preprint arXiv:1611.06355*, 2016.
- A. Radford, L. Metz, and S. Chintala. Unsupervised representation learning with deep convolutional generative adversarial networks. *arXiv preprint arXiv:1511.06434*, 2015.
- P. Ramachandran, B. Zoph, and Q. V. Le. Swish: a self-gated activation function. *arXiv preprint arXiv:1710.05941*, 2017.
- S. Sabour, N. Frosst, and G. E. Hinton. Dynamic routing between capsules. In *Advances in Neural Information Processing Systems*, pages 3859–3869, 2017.
- K. Sohn, H. Lee, and X. Yan. Learning structured output representation using deep conditional generative models. In *Advances in Neural Information Processing Systems*, pages 3483–3491, 2015.
- N. Srivastava and R. R. Salakhutdinov. Multimodal learning with deep boltzmann machines. In *Advances in neural information processing systems*, pages 2222–2230, 2012.
- M. Suzuki, K. Nakayama, and Y. Matsuo. Joint multimodal learning with deep generative models. *arXiv preprint arXiv:1611.01891*, 2016.
- S. Van der Walt, J. L. Schönberger, J. Nunez-Iglesias, F. Boulogne, J. D. Warner, N. Yager, E. Gouillart, and T. Yu. scikit-image: image processing in python. *PeerJ*, 2:e453, 2014.
- R. Vedantam, I. Fischer, J. Huang, and K. Murphy. Generative models of visually grounded imagination. *arXiv preprint arXiv:1705.10762*, 2017.
- O. Vinyals, A. Toshev, S. Bengio, and D. Erhan. Show and tell: A neural image caption generator. In *Computer Vision and Pattern Recognition (CVPR), 2015 IEEE Conference on*, pages 3156–3164. IEEE, 2015.
- W. Wang, X. Yan, H. Lee, and K. Livescu. Deep variational canonical correlation analysis. *arXiv preprint arXiv:1610.03454*, 2016.
- H. Xiao, K. Rasul, and R. Vollgraf. Fashion-mnist: a novel image dataset for benchmarking machine learning algorithms. *arXiv preprint arXiv:1708.07747*, 2017.
- K. Xu, J. Ba, R. Kiros, K. Cho, A. Courville, R. Salakhutdinov, R. Zemel, and Y. Bengio. Show, attend and tell: Neural image caption generation with visual attention. In *International Conference on Machine Learning*, pages 2048–2057, 2015.
- S. Yang, P. Luo, C.-C. Loy, and X. Tang. From facial parts responses to face detection: A deep learning approach. In *Proceedings of the IEEE International Conference on Computer Vision*, pages 3676–3684, 2015.
- I. Yildirim. *From perception to conception: learning multisensory representations*. University of Rochester, 2014.
- S. Zhao, J. Song, and S. Ermon. Towards deeper understanding of variational autoencoding models. *arXiv preprint arXiv:1702.08658*, 2017.